

## *Supporting Information*

# **Double Templating Synthesis of Nanoscale - Spherical Mesoporous Alumina**

### **Instrumental Characterization**

X ray diffraction (XRD, PANalytical X'Pert PRO, Almelo, Holland) and scanning electron microscope (SEM, KYKY-2800B) were used to study the crystallinity and morphology of prepared powders. Transmission electron microscopy (TEM) measurements were carried out on Tecnai G2 F20 operated at 200 kV. All samples were first dispersed in ethanol and then collected by using copper grid covered with carbon films for measurements. Nitrogen sorption isotherms were measured at 77 K on a Micromeritics Tristars 3000 analyzer. Before measurements, the samples were degassed in a vacuum at 180°C for at least 6 h. The Brumauer–Emmett–Teller (BET) method was utilized to calculate the specific surface areas (SBET), using adsorption data in a relative pressure range from 0.04 to 0.2. The pore volume and pore size distributions were derived from the adsorption branches of isotherms by using the Barrett–Joyner–Halenda (BJH) model.

Table S1. Process parameters of alumina

prepared by different reaction temperature and reaction time

Sample number	Urea (g)	Chitin /P123 Weight ratio	Temperature (°C)	Time (h)
---------------	----------	------------------------------	---------------------	----------

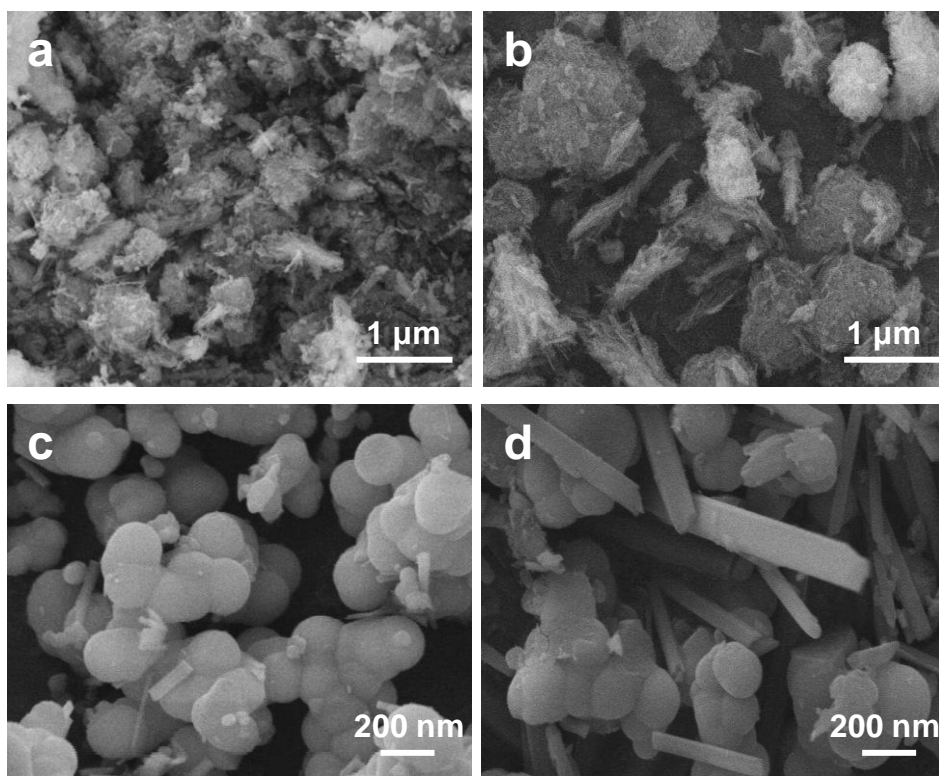
AT1	2.4	3	120	3
BT2	2.4	3	140	3
CT3	2.4	3	160	3
DT4	2.4	3	180	3
ET5	2.4	3	140	9
FT6	2.4	3	140	15

Table S2. Process parameters of spherical alumina prepared by different addition of Chitin powder

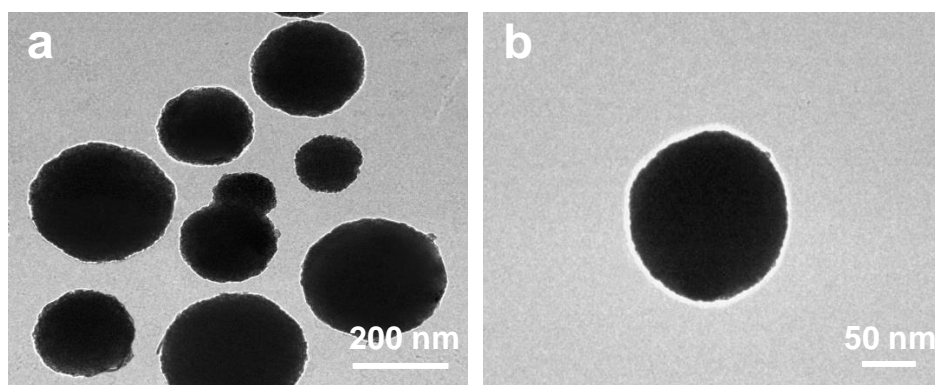
Sample number	Urea (g)	Chitin/P123 Weight ratio	Temperature (°C)	Time (h)
G	2.4	0	140	3
H	2.4	1	140	3
I	2.4	2	140	3
J	2.4	3	140	3
K	2.4	4	140	3

Table S3. Textural properties of mesoporous alumina with different Chitin:P123 weight ratio.

Sample	Weight ratio (Chitin:P123)	Pore size (nm)	Pore volume (cm <sup>3</sup> /g)	BET surface area (m <sup>2</sup> /g)
R <sub>0:4</sub> T <sub>140</sub> H <sub>15</sub>	0:4	7	0.04	99
R <sub>1:1</sub> T <sub>140</sub> H <sub>15</sub>	1:1	7.6	0.17	143
R <sub>2:1</sub> T <sub>140</sub> H <sub>15</sub>	2:1	7.6	0.3	159
R <sub>3:1</sub> T <sub>140</sub> H <sub>15</sub>	3:1	8.6	0.3	184
R <sub>4:1</sub> T <sub>140</sub> H <sub>15</sub>	4:1	5.1	0.23	138



**Figure S1.** Mesoporous alumina samples SEM image prepared under different synthesis conditions: a:  $\text{Al}_2\text{O}_3$ -160-3; b:  $\text{Al}_2\text{O}_3$ -180-3; c:  $\text{Al}_2\text{O}_3$ -140-6; d:  $\text{Al}_2\text{O}_3$ -140-9.



**Figure S2.** TEM images of spherical mesoporous alumina materials.

## Computational details

### Computational methods

We used density functional theory (DFT) executed in the Vienna ab initio simulation package (VASP6.3.3) for all the calculations.<sup>[2-5]</sup> The valence electrons were described by a plane wave basis set with the kinetic cutoff energy of 400 eV, and the core electrons were replaced by the projector augmented wave (PAW) pseudopotentials.<sup>[3,6]</sup> Exchange and correlation were treated within the Perdew-Burke-Ernzerhof (PBE) generalized gradient approximation (GGA).<sup>[7]</sup> The k-point sampling was generated by following the Monkhorst-Pack procedure with a 3×3×1 mesh.<sup>[8]</sup> All structures were calculated until the Hellman-Feynman forces on each ion were lower than 0.03 eV/Å.

The adsorption energy ( $\Delta E_{\text{ads}}$ ) was calculated by using Eq(1), in which  $E_{\text{total}}$  was the total energy of the whole system upon adsorption,  $E_{\text{mol}}$  was the energy of the gas-phase molecule, and  $E_{\text{slab}}$  was the energy of the clean slab.

$$\Delta E_{\text{ads}} = E_{\text{total}} - (E_{\text{slab}} + E_{\text{mol}}) \quad \text{Eq(1)}$$

The differences of charge density ( $\Delta\rho$ ) of CO<sub>2</sub> adsorption were calculated according to the Eq(2).

$$\Delta\rho = \rho_{\text{total}} - (\rho_{\text{slab}} + \rho_{\text{mol}}) \quad \text{Eq(2)}$$

where  $\rho_{\text{total}}$ ,  $\rho_{\text{slab}}$  and  $\rho_{\text{mol}}$  represented the total charge density of CO<sub>2</sub> adsorbed on Al<sub>2</sub>O<sub>3</sub> surface, the charge density of clean Al<sub>2</sub>O<sub>3</sub> surface and CO<sub>2</sub>, respectively.

To evaluate the stability of different facets, we calculated the surface energies ( $\Delta E_{\text{surf}}$ ), see Eq(3):

$$\Delta E_{\text{surf}} = (E_{\text{slab}} - E_{\text{bulk}})/2A \quad \text{Eq(3)}$$

where  $E_{\text{slab}}$  and  $E_{\text{bulk}}$  denoted the energy of Al<sub>2</sub>O<sub>3</sub> surface and bulk, respectively. A was the surface area of clean Al<sub>2</sub>O<sub>3</sub> surface.

### **Theoretical models**

The crystal structures of  $\gamma$ -Al<sub>2</sub>O<sub>3</sub> are complicated. Usually, there are two kinds of structure models used by previous works, namely spinel type and nonspinel type.<sup>[1,9-11]</sup> The defective spinel type gamma-alumina ( $\gamma$ -Al<sub>2</sub>O<sub>3</sub>) as bulky model was chosen in this work.<sup>[12-15]</sup> Similar to previous theoretical works, the "Al<sub>3</sub>O<sub>4</sub>" bulk model was built by replacing all the Mg atoms in the MgAl<sub>2</sub>O<sub>4</sub> (space group: *FD-3M*) by Al atoms.<sup>[16-18]</sup> The optimized lattice constant of resulting "Al<sub>3</sub>O<sub>4</sub>" was a=b=c=8.15 Å, which is in good agreement with previous works. The stoichiometric Al<sub>2</sub>O<sub>3</sub>(110) and Al<sub>2</sub>O<sub>3</sub>(100) surfaces were modeled by (2×1) and (1×2) supercells, respectively. The number of Al and O atoms on both surfaces are 48 and 72. To avoid the artificial interaction between

the repeated slabs along z-direction, 15 Å of vacuum region is introduced.

During the structural relaxation, all the atoms are fully optimized.

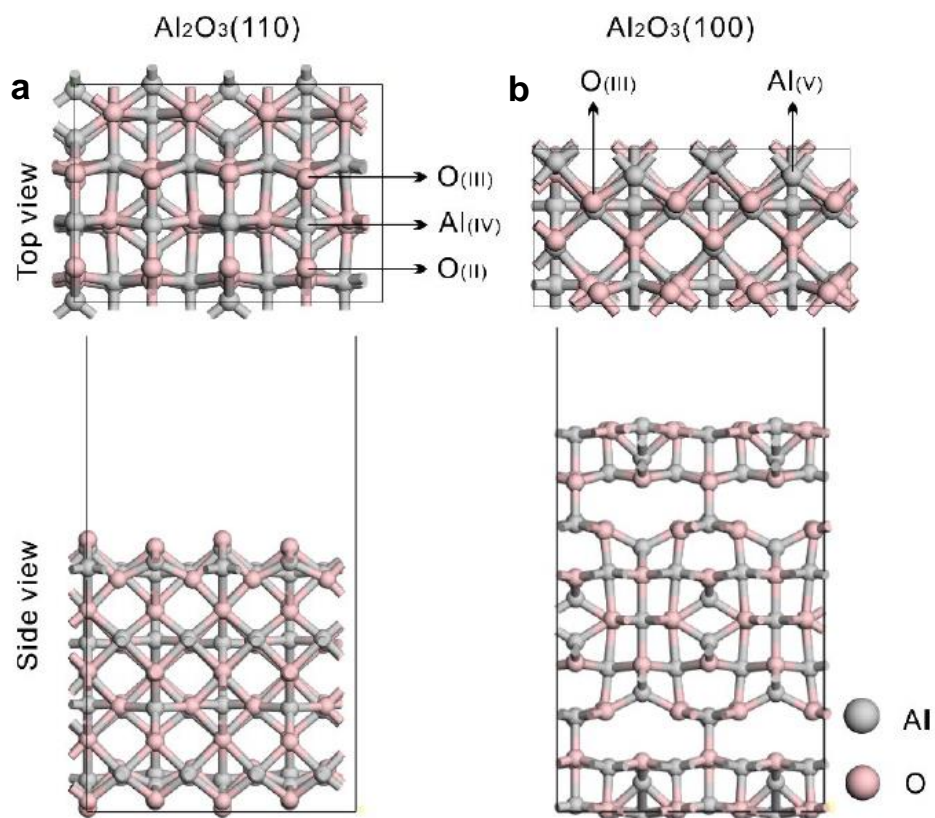


**Figure S3.** The top view and side view of the computational models. (a)

$\text{Al}_2\text{O}_3(110)$  and (b)  $\text{Al}_2\text{O}_3(100)$  surfaces.

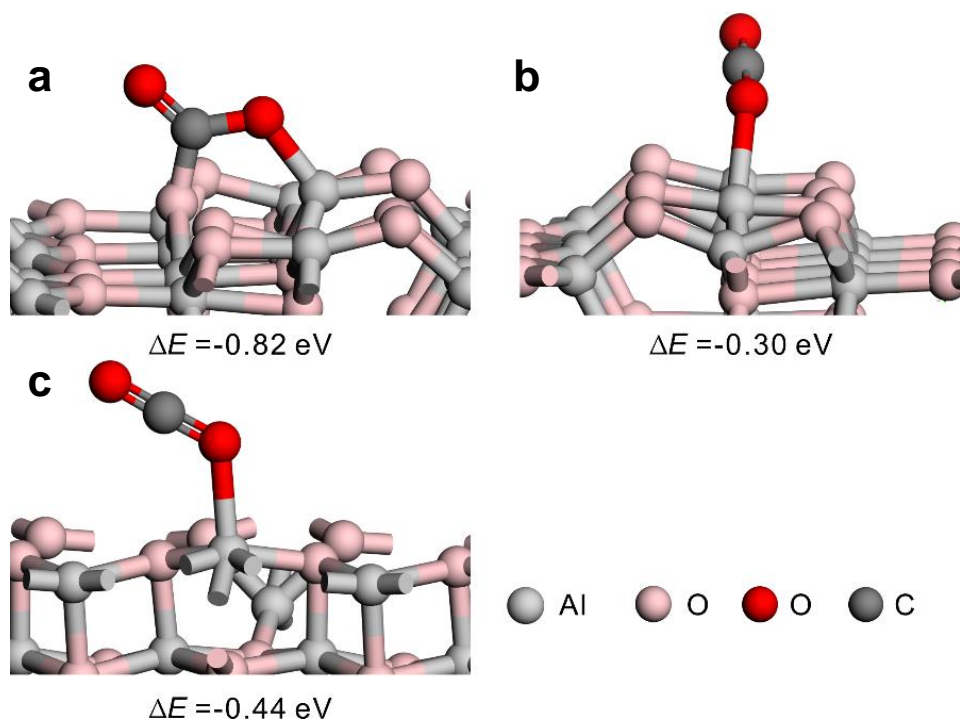


**Figure S4.** The adsorption energies and optimized structures of CO<sub>2</sub> on (a)-  
(b) Al<sub>2</sub>O<sub>3</sub>(110) and (c) Al<sub>2</sub>O<sub>3</sub>(100) surfaces.

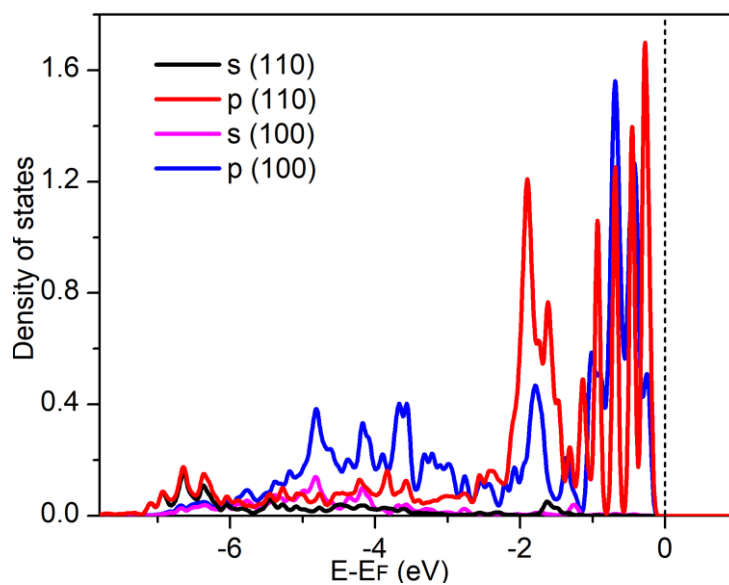


**Figure S5.** Projected density of states (PDOS) of the active sites of Al<sub>(IV)</sub>-O<sub>(II)</sub>  
or Al<sub>(V)</sub>-O<sub>(III)</sub> on Al<sub>2</sub>O<sub>3</sub>(110) and Al<sub>2</sub>O<sub>3</sub>(100), respectively.

## Reference

- [1] M. Digne, P. Sautet, P. Raybaud, P. Euzen, H. Toulhoat, Use of DFT to achieve a rational understanding of acid–basic properties of  $\gamma$ -alumina surfaces, *J. Catal.* 226 (1) (2004) 54-68.
- [2] G. Kresse, J. Hafner, Ab initio molecular-dynamics simulation of the liquid-metal-amorphous-semiconductor transition in germanium, *Phys. Rev. B.* 49 (20) (1994) 14251-14269.
- [3] G. Kresse, J. Hafner, Ab initio molecular dynamics for open-shell transition metals, *Phys. Rev. B.* 48 (17) (1993) 13115-13118.
- [4] G. Kresse, J. Furthmüller, Efficiency of ab-initio total energy calculations for metals and semiconductors using a plane-wave basis set, *Comp. Mater. Sci.* 6 (1) (1996) 15-50.
- [5] G. Kresse, J. Furthmüller, Efficient iterative schemes for ab initio total-energy calculations using a plane-wave basis set, *Phys. Rev. B.* 54 (16) (1996) 11169-11186.
- [6] G. Kresse, D. Joubert, From ultrasoft pseudopotentials to the projector augmented-wave method, *Phys. Rev. B.* 59 (3) (1999) 1758-1775.
- [7] G. Kresse, J. Hafner, Ab initio molecular dynamics for liquid metals, *Phys. Rev. B.* 47 (1) (1993) 558-561.

[8] H.J. Monkhorst, J.D. Pack, Special points for Brillouin-zone integrations, *Phys. Rev. B.* 13 (12) (1976) 5188-5192.

[9] G. Gutiérrez, A. Taga, B. Johansson, Theoretical structure determination of gamma-Al<sub>2</sub>O<sub>3</sub> *Phys. Rev. B.* 65 (1) (2001) 012101.

[10] H.P. Pinto, R.M. Nieminen, S.D. Elliott, Ab initio study of gamma-Al<sub>2</sub>O<sub>3</sub> surfaces, *Phys. Rev. B.* 70 (12) (2004) 125402.

[11] X. Krokidis, P. Raybaud, A.-E. Gobichon, B. Rebours, P. Euzen, H. Toulhoat, Theoretical Study of the Dehydration Process of Boehmite to  $\gamma$ -Alumina, *J. Phys. Chem. B.* 105 (22) (2001) 5121-5130.

[12] G. Gutiérrez, A. Taga, B. Johansson, Theoretical structure determination of  $\gamma$ -Al<sub>2</sub>O<sub>3</sub>, *Phys. Rev. B.* 65 (1) (2001) 012101.

[13] E. Menéndez-Proupin, G. Gutiérrez, Electronic properties of bulk gamma-Al<sub>2</sub>O<sub>3</sub>, *Phys. Rev. B.* 72 (3) (2005) 035116.

[14] W.Y. Ching, L. Ouyang, P. Rulis, H. Yao, Ab initio study of the physical properties of  $\gamma$ -Al<sub>2</sub>O<sub>3</sub>: Lattice dynamics, bulk properties, electronic structure, bonding, optical properties, and ELNES/XANES spectra, *Phys. Rev. B.* 78 (1) (2008) 014106.

[15] A.R. Ferreira, M.J.F. Martins, E. Konstantinova, R.B. Capaz, W.F. Souza, S.S.X. Chiaro, A.A. Leitão, Direct comparison between two  $\gamma$ -alumina structural models by DFT calculations, *J. Solid State Chem.* 184 (5) (2011) 1105-1111.

[16] H.A. Dabbagh, K. Taban, M. Zamani, Effects of vacuum and calcination temperature on the structure, texture, reactivity, and selectivity of alumina: Experimental and DFT studies, *J. Mol. Catal. A: Chem.* 326 (1) (2010) 55-68.

[17] A. Ionescu, A. Allouche, J.-P. Aycard, M. Rajzmann, F. Hutschka, Study of  $\gamma$ -Alumina Surface Reactivity: Adsorption of Water and Hydrogen Sulfide on Octahedral Aluminum Sites, *J. Phys. Chem. B.* 106 (36) (2002) 9359-9366.

[18] A. Ionescu, A. Allouche, J.-P. Aycard, M. Rajzmann, R. Le Gall, Study of  $\gamma$ -Alumina-Supported Hydrotreating Catalyst: I. Adsorption of Bare  $\text{MoS}_2$  Sheets on  $\gamma$ -Alumina Surfaces, *J. Phys. Chem. B.* 107 (33) (2003) 8490-8497.